Table of Contents

Preface

The two fields of Geometric Modeling and Algebraic Geometry, though closely related, are traditionally represented by two almost disjoint scientific communities. Both fields deal with objects defined by algebraic equations, but the objects are studied in different ways. While algebraic geometry has developed impressive results for understanding the theoretical nature of these objects, geometric modeling focuses on practical applications of virtual shapes defined by algebraic equations. Recently, however, interaction between the two fields has stimulated new research. For instance, algorithms for solving intersection problems have benefited from contributions from the algebraic side.

The workshop series on Algebraic Geometry and Geometric Modeling (Vilnius 2002[1], Nice 2004[2]) and on Computational Methods for Algebraic Spline Surfaces (Kefermarkt 2003[3], Oslo 2005) have provided a forum for the interaction between the two fields.

The present volume presents papers from the 2005 Compass workshop, which was aligned with the final review of the European project GAIA II, entitled *Intersection algorithms for geometry based IT-applications using approximate algebraic methods* (IST 2001-35512)[4].

In his invited survey paper, Dokken describes the background, the methods, the results and the achievements of the GAIA project on intersection and implicitization. This project aimed at combining knowledge from Computer Aided Geometric Design, classical algebraic geometry and real symbolic computing to improve intersection algorithms for Computer Aided Design systems. It has produced more than 50 scientific publications and several software toolkits, which are now partly available under the GNU GPL license.

The remaining contributions to this volume can roughly be organized in two groups, which also correspond to the two main activities within the GAIA project. On the one hand, about half of the papers are devoted to the classification of special algebraic surfaces, with particular emphasis on intersections and singularities. On the other hand, several authors report on algorithms for geometric computing – which rely on results from real algebraic geometry – for solving problems such as surface–surface intersection, parameterization, etc.

The first group of contributions consists of the following:

Aries, Briand and Brochou analyze some covariants related to Steiner surfaces, which are the generic case of a quadratically parameterizable quartic surface, frequently used in geometric modeling. More precisely, they exhibit a collection of covariants associated to projective quadratic parameterizations of surfaces with respect to the actions of linear reparameterizations and linear transformations of the target space. Along with

[1] R. Goldman and R. Krasauskas, *Topics in Algebraic Geometry and Geometric Modeling*, Contemporary Mathematics, American Mathematical Society 2003.

[2] M. Elkadi, B. Mourrain and R. Piene, *Algebraic Geometry and Geometric Modeling*, Springer 2006.

[3] T. Dokken and B. Jüttler, *Computational Methods for Algebraic Spline Surfaces*, Springer 2005.

[4] `http://www.sintef.no/IST_GAIA`

the covariants, the authors provide simple geometric interpretations. The results are then used to generate explicit equations and inequalities defining the orbits of projective quadratic parameterizations of quartic surfaces.

Johansen, Løberg and Piene study properties of monoid hypersurfaces – irreducible hypersurfaces of degree d with a singular point of multiplicity $d-1$. Due to the availability of a rational parameterization, these surfaces are of potential interest in computer aided geometric design. The main results include a description of the possible real forms of the singularities on a monoid surface other than the $(d-1)$-uple point. The results are applied to the classification of singularities on quartic monoid surfaces, complementing earlier work on the subject.

Another paper, authored by Breske, Labs and van Straten, is devoted to real line arrangements and surfaces with many real nodes. It is shown that Chmutov's construction for surfaces with many singularities can be modified so as to give surfaces with only real singularities. The results show that all known lower bounds for the number of nodes can be attained with only real singularities. The paper concludes with an application of the theory of real line arrangements which shows that the arrangements used in the paper are asymptotically the best possible ones for the purpose of constructing surfaces with many nodes. This proves a special case of a conjecture of Chmutov.

In their paper, Krasauskas and Zube discuss canal surfaces which are generated as the envelopes of quadratic families of spheres. These surfaces generalize the class of Dupin cyclides, but they are more flexible as blending surfaces between natural quadrics. The authors provide a classification from the point of view of Laguerre geometry and study rational parameterizations of minimal degree, Bézier representations, and implicit equations.

Lê and Galligo present the classification of surfaces of bidegree (1,2) over the field of complex numbers. In particular, the authors study the loci defining self-intersections and singular points in the parameter domain of the surface.

On the other hand, the following papers can be associated with the scond group, which is devoted to algorithmic aspects:

Beck and Schicho discuss the parameterization of planar rational curves over optimal field extensions, by exploiting the Newton polygon. Their method generates a parameterization in a field extension of degree one or two.

Ridges and umbilics of surfaces are among the objects studied in classical differential geometry, and they are of some interest for characterizing and analyzing the shape of a surface. In the case of polynomial parametric surfaces, these special curves are studied in the paper by Cazals et al. In particular, the authors describe an algorithm which generates a certified approximation of the ridges. In order to illustrate the efficiency, the authors report on experiments where the algorithm is applied to Bézier surface patches.

Chau et al. report on several symbolic-numeric techniques for analyzing and computing the intersections and self-intersections of biquadratic tensor product Bézier surface patches. In particular, they explore how far one can go by solely using techniques from symbolic computing, in order to avoid potential robustness problems.

Cube decompositions by eigenvectors of quadratic multivariate splines are analyzed by Ivrissimtzis and Seidel. The results are related to subdivision algorithms, such as the tensor extension of the Doo–Sabin subdivision scheme.

A subdivision method for analyzing the topology of implicitly defined curves in two – and three – dimensional space are studied by Liang, Mourrain and Pavone. The method produces a graph which is isotopic to the curve. The authors also report on implementation aspects and on experiments with planar curves, such as ridge curves or self intersection curves of parameterized surfaces, and on silhouette curves of implicitly defined surfaces.

The final paper of this volume, by Shalaby and Jüttler, describes techniques for the approximate implicitization of space curves and of surfaces of revolution. Both problems can be reduced to the planar situation. Special attention is paid to the problem of unwanted branches and singular points in the region of interest.

The editors are indebted to the reviewers of these proceedings, whose comments have helped greatly to identify the manuscripts suitable for publication, and for improving many of them substantially. Special thanks go to Ms. Bayer for compiling the LaTeX sources into a single coherent manuscript.

Oslo and Linz, *Bert Jüttler*
October 2006 *Ragni Piene*

Ridges and Umbilics of Polynomial Parametric Surfaces

Frédéric Cazals[†], Jean-Charles Faugére[⋆], Marc Pouget[⋆], and Fabrice Rouillier[†]

[†]INRIA Sophia-Antipolis, Geometrica project,
2004 route des Lucioles, BP 93,
F-06902 Sophia-Antipolis, FRANCE.
Frederic.Cazals@sophia.inria.fr
Marc.Pouget@gmail.com
[⋆]INRIA Rocquencourt and
Universit Pierre et Marie Curie-Paris6, UMR 7606, LIP6, Salsa project,
Domaine de Voluceau, BP 105,
F-78153 Le Chesnay Cedex, FRANCE.
Jean-Charles.Faugere@inria.fr
Fabrice.Rouillier@inria.fr

Abstract. Given a smooth surface, a blue (red) ridge is a curve such that at each of its point, the maximum (minimum) principal curvature has an extremum along its curvature line. As curves of *extremal* curvature, ridges are relevant in a number of applications including surface segmentation, analysis, registration, matching. In spite of these interests, given a smooth surface, no algorithm reporting a certified approximation of its ridges was known so far, even for restricted classes of generic surfaces.
This paper partly fills this gap by developing the first algorithm for polynomial parametric surfaces —a class of surfaces ubiquitous in CAGD. The algorithm consists of two stages. First, a polynomial bivariate implicit characterization of ridges $P = 0$ is computed using an implicitization theorem for ridges of a parametric surface. Second, the singular structure of $P = 0$ is exploited, and the approximation problem is reduced to solving zero dimensional systems using Rational Univariate Representations. An experimental section illustrates the efficiency of the algorithm on Bézier patches.

1 Introduction

1.1 Ridges

Originating with the parabolic lines drawn by Felix Klein on the Apollo of Belvedere [10], curves on surfaces have been a natural way to apprehend the aesthetics of shapes [12]. Aside these artistic concerns, applications such as surface segmentation, analysis, registration or matching [11, 16] are concerned with the curves of *extremal curvature* of a surface, which are its so-called *ridges*. (We note in passing that interestingly, (selected) ridges are also central in the analysis of Delaunay based surface meshing algorithms [1].)

A comprehensive literature on ridges exists –see [11, 17, 18], and we just introduce the basic notions so as to discuss our contributions. Consider a smooth embedded

surface whose principal curvatures are denoted k_1 and k_2 with $k_1 \geq k_2$. Away from umbilical points —where $k_1 = k_2$, principal directions of curvature are well defined, and we denote them d_1 and d_2. In local coordinates, we denote $\langle , \rangle$ the inner product induced by the ambient Euclidean space, and the gradients of the principal curvatures are denoted dk_1 and dk_2. Ridges can be defined as follows —see Fig. 1 for an illustration :

Definition 1. *A non umbilical point is called*

- *a blue ridge point if the* extremality coefficient $b_0 = \langle dk_1, d_1 \rangle$ *vanishes, i.e.* $b_0 = 0$.
- *a red ridge point if the* extremality coefficient $b_3 = \langle dk_2, d_2 \rangle$ *vanishes, i.e.* $b_3 = 0$.

As the principal curvatures are not differentiable at umbilics, note that the extremality coefficients are not defined at such points. Notice also the sign of the extremality coefficients is not defined, as each principal direction can be oriented by two opposite unit vectors. Apart from umbilics, special points on ridges are *purple* points –they actually correspond to intersections between red and a blue ridges. The calculation of ridges poses difficulties of three kinds.

Topological difficulties. Ridges of a smooth surface feature self-intersections at umbilics —more precisely at so-called 3-ridges umbilics— and purple points. From a topological viewpoint, reporting a certified approximation of ridges therefore requires reporting these singular points.

Numerical difficulties. As ridges are characterized by derivatives of principal curvatures, reporting them requires evaluating third order differential quantities. Estimating such derivatives depends upon the particular type of surface processed —implicitly defined, parameterized, discretized by a mesh, but is numerically a demanding task.

Orientation difficulties. As observed above, the signs of the b_0 and b_3 depend upon the particular orientations of the principal directions picked. But as a global coherent non vanishing orientation of the principal directions cannot be found in the neighborhoods of umbilics, tracking the zero crossings of b_0 and b_3 faces a major difficulty. For the particular case of surfaces represented by meshes, the so-called *Acute rule* can be used [4], but computing meshes compliant with the requirements imposed by the acute rule is an open problem. For surfaces represented implicitly or parametrically, one can resort to the Gaussian extremality $E_g = b_0 b_3$, which eradicates the sign problems, but prevents from reporting the red and blue ridges separately.

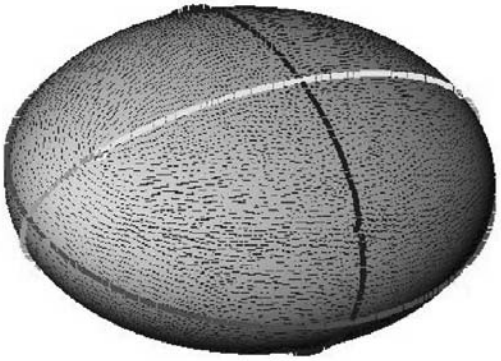

Fig. 1. Umbilics, ridges, and principal blue foliation on the ellipsoid for normals pointing outward

1.2 Previous work

Given the previous difficulties, no algorithm reporting ridges in a certified fashion had been developed until this work. Most contributions deal with sampled surfaces known through a mesh, and a complete review of these contributions can be found in [4]. In the following, we focus on contributions related to parametric surfaces.

Reporting umbilics. Umbilics of a surface are always traversed by ridges, so that reporting ridges faithfully requires reporting umbilics. To do so, Morris [13] minimizes the function $k_1 - k_2$, which vanishes exactly at umbilics. Meakawa et al. [15] define a polynomial system whose roots are the umbilics. This system is solved with the *rounded interval arithmetic projected polyhedron method*. This algorithm uses specific properties of the Bernstein basis of polynomials and interval arithmetic. The domain is recursively subdivided and a set of boxes containing the umbilics is output, but neither existence nor uniqueness of an umbilic in a box is guaranteed.

Reporting ridges. The only method dedicated to parametric surfaces we are aware of is that of Morris [13, 14]. The parametric domain is triangulated and zero crossings are sought on edges. Local orientation of the principal directions are needed but only provided with a heuristic. This enables to detect crossings assuming (i)there is at most one such crossing on an edge (ii)the orientation of the principal directions is correct. As this simple algorithm fails near umbilics, these points are located first and crossings are found on a circle around the umbilic.

Equation of the ridge curve. Ridges can be characterized either as extrema of principal curvatures along their curvature lines as in definition 1, or by analyzing the contact between the surface and spheres [11]. For parametric surfaces, this later approach allows a global characterization of ridges [18, Chapter 11] as a 1 dimensional smooth sub-manifold in a 7 dimensional space. But this characterization is not amenable to algorithmic developments.

Shifting from this seven-dimensional space to the parametric space, the theory of algebraic invariants has been used to derive the equation of the ridge curve as the zero

set of an invariant function [8]. The ensuing strategy consists of defining invariants as functions of the fundamental forms and their derivatives. The equation of ridges is given in this setting. If one further specializes this equation for a surface given by a parameterization, the result matches, up to a constant factor, our implicit encoding $P = 0$ [3]. The point of view of our approach is to work from the beginning on a parametrized surface. The definition of ridges involves principal curvatures and principal directions of curvature which are independent of the given parametrization, but we explicit all these invariants wrt the parametrization and its derivatives. Hence, for polynomial parametric surfaces, we end with a polynomial with integer coefficients whose variables are the partial derivatives of the parametrization up to the third order. This polynomial is the same for any other parametrization.

Reporting the topology of an algebraic curve. In the case of a polynomial parametric surface, we recast the problem of approximating ridges into the field of algebraic geometry. We recall that the standard tool to compute a graph encoding the topology of a 2-D or 3-D curve is the Cylindrical Algebraic Decomposition (CAD) [7, 9].

1.3 Contributions and paper overview

Let $\Phi(u, v)$ be a smooth parameterized surface over a domain $\mathcal{D} \subset \mathbb{R}^2$. We wish to report a certified approximation of its ridges, which subsumes a solution for all the difficulties enumerated in section 1.1.

The first step in providing a certified approximation of the ridges of Φ consists of computing an implicit equation $P = 0$ encoding these ridges. The derivation of this equation is presented in the companion paper [3], which also contains a detailed discussion of our implicit encoding of ridges wrt previous work.

The equation $P = 0$ being taken for granted, the contribution developed in this paper is to exploit as far as possible the geometry of $\mathcal{P}$ encoded in $P = 0$, so as to develop the first algorithm able to compute the ridges topology of a polynomial parametric surface. Our algorithm avoids the main difficulties of CAD methods: (i) singular and critical points are sequentially computed directly in $2D$; (ii) no generic assumption is required, i.e. several critical or singular points may have the same horizontal projection; (iii) no computation with algebraic numbers is involved. Because algorithms based on the Cylindrical Algebraic Decomposition are not effective for our high degree curves such as $P = 0$, our algorithm is to the best of our knowledge the only one able to certify properties of the curve $P = 0$.

The paper is organized as follows. The implicit equations for ridges and its singularities are recalled in section 2. The algorithm to compute the topology of the ridge curve is described in section 3. Section 4 provides illustrations on two Bézier surfaces.

1.4 Notations

Ridges and umbilics. At any non umbilical point of the surface, the maximal (minimal) principal curvature is denoted k_1 (k_2), and its associated direction d_1 (d_2). Anything related to the maximal (minimal) curvature is qualified blue (red), for example we shall

speak of the blue curvature for k_1 or the red direction for d_2. Since we shall make precise statements about ridges, it should be recalled that, according to definition 1, umbilics are not ridge points.

Differential calculus. For a bivariate function $f(u,v)$, the partial derivatives are denoted with indices, for example $f_{uuv} = \frac{\partial^3 f}{\partial^2 u \partial v}$. The gradient of f is denoted f_1 or $df = (f_u, f_v)$. The quadratic form induced by the second derivatives is denoted $f_2(u,v) = f_{uu}u^2 + 2f_{uv}uv + f_{vv}v^2$. The discriminant of this form is denoted $\delta(f_2) = f_{uv}^2 - f_{uu}f_{vv}$. The cubic form induced by the third derivatives in denoted $f_3(u,v) = f_{uuu}u^3 + 3f_{uuv}u^2v + 3f_{uvv}uv^2 + f_{vvv}v^3$. The discriminant of this form is denoted $\delta(f_3) = 4(f_{uuu}f_{uvv} - f_{uuv}^2)(f_{uuv}f_{vvv} - f_{uvv}^2) - (f_{uuu}f_{vvv} - f_{uuv}f_{uvv})^2$.

Let f be a real bivariate polynomial and $\mathcal{F}$ the real algebraic curve defined by f. A point $(u,v) \in \mathbb{C}^2$ is called

- a singular point of $\mathcal{F}$ if $f(u,v) = 0$, $f_u(u,v) = 0$ and $f_v(u,v) = 0$;
- a critical point of $\mathcal{F}$ if $f(u,v) = 0$, $f_u(u,v) = 0$ and $f_v(u,v) \neq 0$ (such a point has an horizontal tangent, we call it critical because if one fixes the v coordinate, then the restricted function is critical wrt the u coordinate, this notion will be useful in section 3);
- a regular point of $\mathcal{F}$ if $f(u,v) = 0$ and it is neither singular nor critical.

If the domain $\mathcal{D}$ of study is a subset of $\mathbb{R}^2$, one calls fiber a cross section of this domain at a given ordinate or abscissa.

Misc. The inner product of two vectors x, y is denoted $\langle x, y \rangle$.

2 Relevant equations for ridges and its singularities

This section briefly recalls the equations defining the ridge curve and its singularities, see [3]. Let Φ be the parameterization of class C^k for $k \geq 4$. Denote I and II the matrices of the first and second fundamental form of the surface in the basis (Φ_u, Φ_v) of the tangent space. In order for normals and curvatures to be well defined, we assume the surface is regular i.e. $\det(I) \neq 0$.

The principal directions d_i and principal curvatures $k_1 \geq k_2$ are the eigenvectors and eigenvalues of the matrix $W = I^{-1}II$. The following equation defines coefficients A, B, C and D as polynomials wrt the derivative of the parameterization Φ up to the second order

$$\begin{pmatrix} A & B \\ C & D \end{pmatrix} = W(\det I)^{3/2}. \tag{1}$$

As a general rule, in the following calculations, we will be interested in deriving quantities which are polynomials wrt the derivatives of the parameterization. These calculations are based on quantities (principal curvatures and directions) which are independent of a given parameterization, hence the derived formula are valid for any parameterization.

Umbilics are characterized by the equation $p_2 = 0$, with $p_2 = (k_1 - k_2)^2(\det I)^3$.

We then define two vector fields v_1 and w_1 orienting the principal direction field d_1

$$v_1 = (-2B, A - D - \sqrt{p_2})$$
$$w_1 = (A - D + \sqrt{p_2}, 2C).$$

Derivatives of the principal direction k_1 wrt these two vector fields define a, a', b, b' by the equations:

$$a\sqrt{p_2}+b = \sqrt{p_2}(\det I)^{5/2}\langle\, dk_1, v_1\,\rangle\,; \quad a'\sqrt{p_2}+b' = \sqrt{p_2}(\det I)^{5/2}\langle\, dk_1, w_1\,\rangle. \quad (2)$$

The following definition is a technical tool to state the next theorem in a simple way. The function $Sign_{ridge}$ introduced here will be used to classify ridge colors. Essentially, this function describes all the possible sign configurations for ab and $a'b'$ at a ridge point.

Definition 2. *The function $Sign_{ridge}$ takes the values*

$$\textit{-1 if} \begin{cases} ab < 0 \\ a'b' \le 0 \end{cases} \textit{ or } \begin{cases} ab \le 0 \\ a'b' < 0 \end{cases},$$
$$\textit{+1 if} \begin{cases} ab > 0 \\ a'b' \ge 0 \end{cases} \textit{ or } \begin{cases} ab \ge 0 \\ a'b' > 0 \end{cases},$$
$$\textit{0 if } ab = a'b' = 0.$$

Theorem 3. *The set of blue ridges union the set of red ridges union the set of umbilics has equation $P = 0$ where $P = (a^2p_2 - b^2)/B$ is a polynomial wrt $A, B, C, D, \det I$ as well as their first derivatives and hence is a polynomial wrt the derivatives of the parameterization up to the third order. For a point of this set $\mathcal{P}$, one has:*

- *If $p_2 = 0$, the point is an umbilic.*
- *If $p_2 \neq 0$ then:*
  - *if $Sign_{ridge} = -1$ then the point is a blue ridge point,*
  - *if $Sign_{ridge} = +1$ then the point is a red ridge point,*
  - *if $Sign_{ridge} = 0$ then the point is a purple point.*

In addition, the classification of an umbilic as 1-ridge or 3-ridges from P_3 goes as follows:

- If P_3 is elliptic, that is the discriminant of P_3 is positive ($\delta(P_3) > 0$), then the umbilic is a 3-ridge umbilic and the 3 tangent lines to the ridges at the umbilic are distinct.
- If P_3 is hyperbolic ($\delta(P_3) < 0$) then the umbilic is a 1-ridge umbilic.

2.1 Polynomial surfaces

A fundamental class of surface used in Computer Aided Geometric Design consists of polynomial surfaces like Bézier and splines. We first observe that if Φ is a polynomial, all its derivatives are also polynomials. Thus in the polynomial case the equation of

ridges, which is a polynomial wrt to these derivatives, is algebraic. Hence the set of all ridges and umbilics is globally described by an algebraic curve. Notice that the parameterization can be general, in which case $\Phi(u,v) = (x(u,v), y(u,v), z(u,v))$, or can be a height function $\Phi(u,v) = (u, v, z(u,v))$.

As a corollary of Thm. 3, one can give upper bounds for the total degree of the polynomial P wrt that of the parameterization. Distinguishing the cases where Φ is a general parameterization or a height function (that is $\Phi(u,v) = (u, v, h(u,v))$) with $h(u,v)$ and denoting d the total degree of Φ, P has total degree $33d - 40$ or $15d - 22$ for a height function.

In the more general case where the parameterization is given by rational fractions of polynomials, P is a rational function of the surface parameters too. The denominator of P codes the points where the surface is not defined and away from these points, the numerator codes the ridges and umbilics.

3 Certified topological approximation

In this section, we circumvent the difficulties of the Cylindrical Algebraic Decomposition (CAD) and develop a certified algorithm to compute the topology of $\mathcal{P}$. Consider a parameterized surface $\Phi(u,v)$, the parameterization being *polynomial* with rational coefficients. Let $\mathcal{P}$ be the curve encoding the ridges of $\Phi(u,v)$. We aim at studying $\mathcal{P}$ on the compact box domain $\mathcal{D} = [a,b] \times [c,d]$.

Given a real algebraic curve, the standard way to approximate it consists of resorting to the CAD. Running the CAD requires computing singular points and critical points of the curve —points with a horizontal tangent. Theoretically, these points are defined by zero-dimensional systems. Practically, because of the high degree of the polynomials involved, the calculations may not go through. Replacing the bottlenecks of the CAD by a resolution method adapted to the singular structure of $\mathcal{P}$, we develop an algorithm producing a graph $\mathcal{G}$ embedded in the domain $\mathcal{D}$, which is isotopic to the curve $\mathcal{P}$ of ridges in $\mathcal{D}$. Key points are that:

1. no generic assumption is required, i.e. several critical or singular points may have the same horizontal projection;
2. no computation with algebraic numbers is involved.

3.1 Algebraic tools

Two algebraic methods are ubiquitously called by our algorithm: univariate root isolation and rational univariate representation. We briefly present these tools and give references for the interested reader.

Univariate root isolation. This tool enables to isolate roots of univariate polynomials whose coefficients are rational numbers, by means of intervals with rational bounds. The method uses the Descartes rule and is fully explained in [20].

Rational univariate representation [19]. The Rational Univariate Representation is, with the end-user point of view, the simplest way for representing symbolically the roots of a zero-dimensional system without loosing information (multiplicities or real

roots) since one can get all the information on the roots of the system by solving univariate polynomials.

Given a zero-dimensional system

$$I =< p_1, \ldots, p_s >$$

where the $p_i \in \mathbb{Q}[X_1, \ldots, X_n]$, a Rational Univariate Representation of $\mathrm{V}(I)$, has the following shape:

$$f_t(T) = 0, X_1 = \frac{g_{t,X_1}(T)}{g_{t,1}(T)}, \ldots, X_n = \frac{g_{t,X_n}(T)}{g_{t,1}(T)},$$

where $f_t, g_{t,1}, g_{t,X_1}, \ldots, g_{t,X_n} \in \mathbb{Q}[T]$ (T is a new variable). It is uniquely defined w.r.t. a given polynomial t which separates $V(I)$ (injective on $V(I)$), the polynomial f_t being necessarily the characteristic polynomial of m_t in $\mathbb{Q}[X_1, \ldots, X_n]/I$. The RUR defines a one-to-one map between the roots of I and those of f_t preserving the multiplicities and the real roots :

$$\begin{array}{ccc} \mathrm{V}(I)(\cap\mathbb{R}) & \approx & \mathrm{V}(f_t)(\cap\mathbb{R}) \\ \alpha = (\alpha_1, \ldots, \alpha_n) & \rightarrow & t(\alpha) \\ (\frac{g_{t,X_1}(t(\alpha))}{g_{t,1}(t(\alpha))}, \ldots, \frac{g_{t,X_n}(t(\alpha))}{g_{t,1}(t(\alpha))}) & \leftarrow & t(\alpha) \end{array}$$

The RUR also enables efficient evaluation of the sign of polynomials at the roots of a system.

3.2 Assumptions on the ridge curve and study points

According to the structure of the singularities of the ridge curve recalled in section 2, the only assumption made is that the surface admits generic ridges in the sense that real singularities of $\mathcal{P}$ satisfy the following conditions:

- Real singularities of $\mathcal{P}$ are of multiplicity at most 3.
- Real singularities of multiplicity 2 are called purple points. They satisfy the system $S_p = \{a = b = a' = b' = 0,\ \delta(P_2) > 0,\ p_2 \neq 0\}$. In addition, this implies that two real branches of $\mathcal{P}$ are passing through a purple point.
- Real singularities of multiplicity 3 are called umbilics and they satisfy the system $S_u = \{p_2 = 0\} = \{p_2 = 0, P = 0, P_u = 0, P_v = 0\}$. In addition, if $\delta(P_3)$ denote the discriminant of the cubic of the third derivatives of P at an umbilic, one has:
  - if $\delta(P_3) > 0$, then the umbilic is called a 3-ridge umbilic and three real branches of $\mathcal{P}$ are passing through the umbilic with three distinct tangents;
  - if $\delta(P_3) < 0$, then the umbilic is called a 1-ridge umbilic and one real branch of $\mathcal{P}$ is passing through the umbilic.

As we shall see in section 3.5, these conditions are checked during the processing of the algorithm.

Given this structure of singular points, the algorithm successively isolate umbilics, purple points and critical points. As a system defining one set of these points also includes the points of the previous system, we use a localization method to simplify

the calculations. The points reported at each stage are characterized as roots of a zero-dimensional system —a system with a finite number of complex solutions, together with the number of half-branches of the curve connected to each point. In addition, points on the border of the domain of study need a special care. This setting leads to the definition of *study points*:

Definition 4. *Study points are points in $\mathcal{D}$ which are*

- *real singularities of $\mathcal{P}$, that is $S_s = S_u \cup S_p$, with $S_u = S_{1R} \cup S_{3R}$ and*
  - $S_{1R} = \{p_2 = P = P_u = P_v = 0, \delta(P_3) < 0\}$
  - $S_{3R} = \{p_2 = P = P_u = P_v = 0, \delta(P_3) > 0\}$
  - $S_p = \{a = b = a' = b' = 0,\ \delta(P_2) > 0,\ p_2 \neq 0\}$
    $= \{a = b = a' = b' = 0,\ \delta(P_2) > 0\} \setminus S_u$
- *real critical points of $\mathcal{P}$ in the v-direction (i.e. points with a horizontal tangent which are not singularities of $\mathcal{P}$) defined by the system*
  $S_c = \{P = P_u = 0, P_v \neq 0\}$*;*
- *intersections of $\mathcal{P}$ with the left and right sides of the box $\mathcal{D}$ satisfying the system* $S_b = \{P(a, v) = 0,\ v \in [c, d]\} \cup \{P(b, v) = 0,\ v \in [c, d]\}$*. Such a point may also be critical or singular.*

3.3 Output specification

Definition 5. *Let $\mathcal{G}$ be a graph whose vertices are points of $\mathcal{D}$ and edges are non-intersecting straight line-segments between vertices. Let the topology on $\mathcal{G}$ be induced by that of $\mathcal{D}$. We say that $\mathcal{G}$ is a topological approximation of the ridge curve $\mathcal{P}$ on the domain $\mathcal{D}$ if $\mathcal{G}$ is ambient isotopic to $\mathcal{P} \cap \mathcal{D}$ in $\mathcal{D}$.*

More formally, there exists a function $F : \mathcal{D} \times [0, 1] \longrightarrow \mathcal{D}$ such that:

- *F is continuous;*
- *$\forall t \in [0, 1],\ F_t = F(., t)$ is an homeomorphism of $\mathcal{D}$ onto itself;*
- *$F_0 = Id_{\mathcal{D}}$ and $F_1(\mathcal{P} \cap \mathcal{D}) = \mathcal{G}$.*

Note that homeomorphic approximation is weaker and our algorithm actually gives isotopy. In addition, our construction allows to identify singularities of $\mathcal{P}$ to a subset of vertices of $\mathcal{G}$ while controlling the error on the geometric positions. We can also color edges of $\mathcal{G}$ with the color of the ridge curve it is isotopic to. Once this topological sketch is given, one can easily compute a more accurate geometrical picture.

3.4 Method outline

Taking the square free part of P, we can assume P is square free. We can also assume $\mathcal{P}$ has no part which is a horizontal segment —parallel to the u-axis. Otherwise this means that a whole horizontal line is a component of P. In other words, the content of P wrt u is a polynomial in v and we can study this factor separately and divide P by this factor. Eventually, to get the whole topology of the curve, one has to merge the components.

Our algorithms consists of the following five stages:

1. **Isolating study points.** Study point are isolated in $2D$ with rational univariate representations (RUR). Study points within a common fiber are identified.
2. **Regularization of the study boxes.** We know the number of branches of the curve going through each study point. The boxes of study points are reduced so as to be able to define the number of branches coming from the bottom and from the top.
3. **Computing regular points in study fibers.** In each fiber of a study point, the u-coordinates of intersection points with $\mathcal{P}$ other than study points are computed.
4. **Adding intermediate rational fibers.** Add rational fibers between study points fibers and isolate the u-coordinates of intersection points with $\mathcal{P}$.
5. **Performing connections.** This information is enough to perform the connections. Consider the cylinder between two consecutive fibers, the number of branches connected from above the lower fiber is the same than the number of branches connected from below the higher fiber. Hence there is only one way to perform connections with non-intersecting straight segments.

3.5 Step 1. Isolating study points

The method to identify these study points is to compute a RUR of the system defining them. More precisely, we sequentially solve the following systems:

1. The system S_u from which the sets S_{1R} and S_{3R} are distinguished by evaluating the sign of $\delta(P_3)$.
2. The system S_p for purple points.
3. The system S_c for critical points.
4. The system S_b for border points, that is intersections of $\mathcal{P}$ with the left and right sides of the box $\mathcal{D}$. Solving this system together with one of the previous identifies border points which are also singular or critical.

Selecting only points belonging to $\mathcal{D}$ reduces to adding inequalities to the systems and is well managed by the RUR. According to [19], solving such systems is equivalent to solving zero-dimensional systems without inequalities when the number of inequations remains small compared to the number of variables. The RUR of the study points provides a way to compute a box around each study point q_i which is a product of two intervals $[u_i^1; u_i^2] \times [v_i^1; v_i^2]$. The intervals can be as small as desired.

Until now, we only have separate information on the different systems. In order to identify study points having the same v-coordinate, we need to cross this information. First we compute isolation intervals for all the v-coordinates of all the study points together, denote I this list of intervals. If two study points with the same v-coordinate are solutions of two different systems, the gcd of polynomials enable to identify them:

– Initialize the list I with all the isolation intervals of all the v-coordinates of the different systems.
– Let A and B be the square free polynomials defining the v-coordinates of two different systems, and $I_A,\ I_B$ the lists of isolation intervals of their roots. Let $C = gcd(A, B)$ and I_C the list of isolation intervals of its roots. One can refine the elements of I_C until they intersect only one element of I_A and one element of I_B. Then replace these two intervals in I by the single interval which is the intersection of the three intervals. Do the same for every pair of systems.

– I then contains intervals defining different real numbers in one-to-one correspondence with the v-coordinates of the study points. It remains to refine these intervals until they are all disjoint.

Second, we compare the intervals of I and those of the 2d boxes of the study points. Let two study points q_i and q_j be represented by $[u_i^1; u_i^2] \times [v_i^1; v_i^2]$ and $[u_j^1; u_j^2] \times [v_j^1; v_j^2]$ with $[v_i^1; v_i^2] \cap [v_j^1; v_j^2] \neq \varnothing$. One cannot, a priori, decide if these two points have the same v-coordinate or if a refinement of the boxes will end with disjoint v-intervals. On the other hand, with the list I, such a decision is straightforward. The boxes of the study points are refined until each $[v_i^1; v_i^2]$ intersects only one interval $[w_i^1; w_i^2]$ of the list I. Then two study points intersecting the same interval $[w_i^1; w_i^2]$ are in the same fiber.

Finally, one can refine the u-coordinates of the study points with the same v coordinate until they are represented with disjoint intervals since, thanks to localizations, all the computed points are distinct.

Checking genericity conditions of section 3.2.

First, real singularities shall be the union of purple and umbilical points, this reduces to compare the systems for singular points and for purple and umbilical points. Second, showing that $\delta(P_3) \neq 0$ for umbilics and $\delta(P_2) > 0$ for purple points reduces to sign evaluation of polynomials at the roots of a system (see section 3.1).

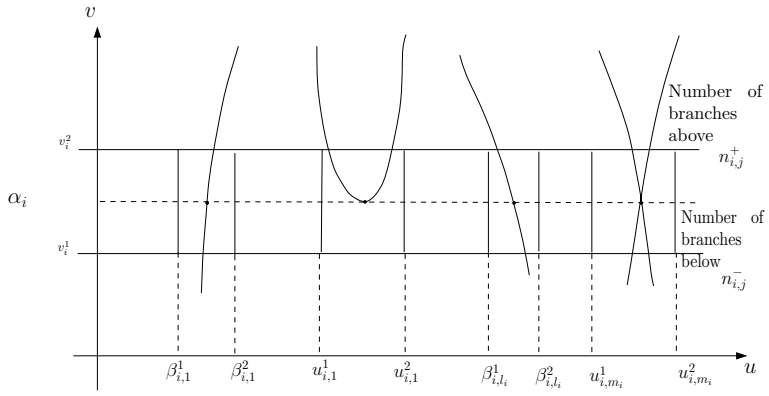

Fig. 2. Notations for a fiber involving several critical/singular points: $u_{i,j}^{1(2)}$ are used for study points, $\beta_{i,j}^{1(2)}$ for simple points.

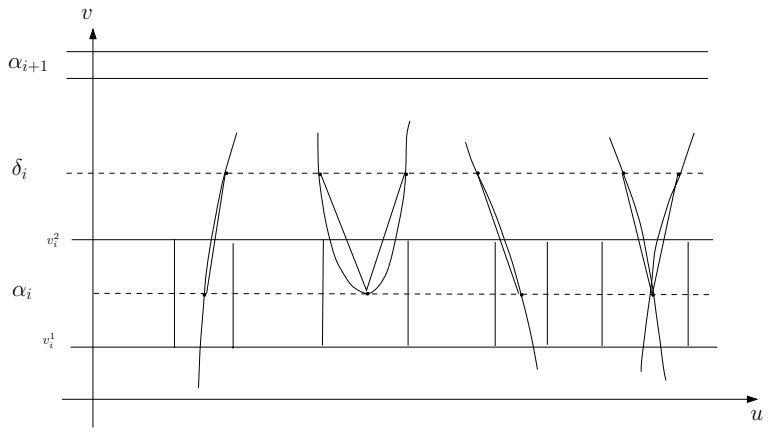

Fig. 3. Performing connections between the study point fiber α_i and the intermediate fiber δ_i

3.6 Step 2. Regularization of the study boxes

At this stage, we have computed isolating boxes of all study points $\{q_{i,j}, i = 1 \dots s, j = 1 \dots m_i\}$: the v-coordinates $\alpha_1, ..., \alpha_s$ are isolated by intervals $[v_i^1; v_i^2], i = 1..s$ and the u-coordinates of the m_i study points in each fiber α_i are isolated by intervals $[u_{i,j}^1; u_{i,j}^2], j = 1..m_i$.

We know the number of branches of the curve passing through each study point : it is 6 for a 3-ridge umbilic, 4 for a purple and 2 for others. We want to compute the number branches coming from the bottom and from the top. We first reduce the box until the number of intersections between the curve and the border of the box matches the known number of branches connected to the study point. Then the intersections are obviously in one-to-one correspondence with the branches. Second, as in [21] for example, we reduce the height of the box again if necessary so that intersections only occur on the top or the bottom of the box.

Counting the number of intersections reduces to solve 4 univariate polynomials with rational coefficients. Reducing a box means refining its representation with the RUR.

3.7 Step 3. Computing regular points in study fibers

We now compute the regular points in each fiber $P(u, \alpha_i) = 0$. Computing the regular points of each fiber is now equivalent to computing the roots of the polynomials $P(u, \alpha_i)$ outside the intervals representing the u-coordinates of the study points (which contain all the multiple roots of $P(u, \alpha_i)$).

Denote $[u_{i,j}^1; u_{i,j}^2], j = 1..m_i$ the intervals representing the u-coordinates of the study points on the fiber of α_i and $[v_i^1, v_i^2]$ an interval containing (strictly) α_i and no other $\alpha_j, j \neq i$. Substituting v by any rational value $q \in [v_i^1, v_i^2]$ in $P(u, v)$ gives a univariate polynomial with rational coefficients $P(u, q)$. We then isolate the (simple) roots of this polynomial $P(u, q)$ on the domain $[a, b] \setminus \cup_{j=1}^{m_i} [u_{i,j}^1; u_{i,j}^2]$: the algorithm returns intervals $[\beta_{i,j}^1; \beta_{i,j}^2], j = 1 \dots l_i$ representing these roots.

To summarize the information up to this point : we have, along each fiber, a collection of points $s_{i,j}$, $i = 1 \dots s,\ j = 1, \dots, m_i + l_i$, which are either study points or regular points of $\mathcal{P}$. Each such point is isolated in a box i.e. a product of intervals and comes with two integers $(n^+_{i,j}, n^-_{i,j})$ denoting the number of branches in $\mathcal{D}$ connected from above and from below.

3.8 Step 4. Adding intermediate rational fibers

Consider now an intermediate fiber, i.e. a fiber associated with $v = \delta_i\ i = 1 \dots s-1$, with δ_i a rational number in-between the intervals of isolation of two consecutive values α_i and α_{i+1}. If the fibers $v = c$ or $v = d$ are not fibers of study points, then they are added as fibers δ_0 or δ_s.

Getting the structure of such fibers amounts to solving a univariate polynomial with rational coefficients, which is done using the algorithm described in section 3.1. Thus, each such fiber also comes with a collection of points, isolated in boxes, for which one knows that $n^+_{i,j} = n^-_{i,j} = 1$.

3.9 Step 5. Performing connections

We thus obtain a full and certified description of the fibers: all the intersection points with $\mathcal{P}$ and their number of branches connected. We know, by construction, that the branches of $\mathcal{P}$ between fibers have empty intersection. The number of branches connected from above a fiber is the same than the number of branches connected from below the next fiber. Hence there is only one way to perform connections with non-intersecting straight segments. More precisely, vertices of the graph are the centers of isolation boxes, and edges are line-segments joining them.

Notice that using the intermediate fibers $v = \delta_i$ is compulsory if one wishes to get a graph $\mathcal{G}$ isotopic to $\mathcal{P}$. If not, whenever two branches have common starting points and endpoints, the embedding of the graph $\mathcal{G}$ obtained is not valid since two arcs are identified.

The algorithm is illustrated on Fig. 3. In addition

- If a singular point box have width δ, then the distance between the singular point and the vertex representing it is less than δ.
- One can compute the sign of the function $Sign_{ridge}$ (definition 2) for each regular point of each intermediate fiber. This defines the color of the ridge branch it belongs to. Then one can assign to each edge of the graph the color of its end point which is on an intermediate fiber.

4 Illustration

We provide the topology of ridges for two Bézier surfaces defined over the domain $\mathcal{D} = [0,1] \times [0,1]$.

The first surface has control points

$$\begin{pmatrix} [0,0,0] & [1/4,0,0] & [2/4,0,0] & [3/4,0,0] & [4/4,0,0] \\ [0,1/4,0] & [1/4,1/4,1] & [2/4,1/4,-1] & [3/4,1/4,-1] & [4/4,1/4,0] \\ [0,2/4,0] & [1/4,2/4,-1] & [2/4,2/4,1] & [3/4,2/4,1] & [4/4,2/4,0] \\ [0,3/4,0] & [1/4,3/4,1] & [2/4,3/4,-1] & [3/4,3/4,1] & [4/4,3/4,0] \\ [0,4/4,0] & [1/4,4/4,0] & [2/4,4/4,0] & [3/4,4/4,0] & [4/4,4/4,0] \end{pmatrix}$$

Alternatively, this surface can be expressed as the graph of the total degree 8 polynomial $h(u,v)$ for $(u,v) \in [0,1]^2$:

$$h(u,v) = 116u^4v^4 - 200u^4v^3 + 108u^4v^2 - 24u^4v - 312u^3v^4 + 592u^3v^3 - 360u^3v^2 + 80u^3v + 252u^2v^4 - 504u^2v^3 + 324u^2v^2 - 72u^2v - 56uv^4 + 112uv^3 - 72uv^2 + 16uv.$$

The computation of the implicit curve has been performed using Maple 9.5 and requires less than one minute (see [3]). It is a bivariate polynomial $P(u,v)$ of total degree 84, of degree 43 in u, degree 43 in v with 1907 terms and coefficients with up to 53 digits. Figure 4 displays the topological approximation graph of the ridge curve in the parametric domain $\mathcal{D}$ computed with the algorithm of section 3. There are 19 critical points (black dots), 17 purple points (pink dots) and 8 umbilics, 3 of which are 3-ridge (green) and 5 are 1-ridge (yellow).

We have computed the subsets S_u, S_p and S_c by using the software FGB and RS (`http://fgbrs.lip6.fr`). The RUR can be computed as shown in [19] or alternatively, Gröbner basis can be computed first using [5] or [6]. We tested both methods and the computation time for the biggest system S_c does not exceed 10 minutes with a Pentium M 1.6 Ghz. The following table gives the main characteristics of these systems :

System	# of roots $\in \mathbb{C}$	# of roots $\in \mathbb{R}$	# of real roots $\in \mathcal{D}$
S_u	160	16	8
S_p	749	47	17
S_c	1432	44	19

In order to have more insight of the geometric meaning of the ridge curve, the surface and its ridges are displayed on Fig. 5. This plot is computed without topological certification with the `rs_tci_points` function (from RS software, see also [2]) from the polynomial P and then lifted on the surface.

The second surface is a bi-quadratic Bézier of equation

$$\begin{aligned} \Phi(u,v) = [&2/3\,v + 2/3\,uv - 1/3\,u^2v + 1/3\,v^2 - 2/3\,v^2u + 1/3\,u^2v^2, \\ &1/2\,u + 1/2\,u^2 + uv - u^2v - 1/2\,v^2u + 1/2\,u^2v^2, \\ &1 + 3\,v^2 - u - 4\,v + 5\,uv + u^2v - 7/2\,v^2u - 5/2\,u^2v^2] \end{aligned}$$

The ridge curve has total degree 56 and partial degrees 33 with 1078 terms and coefficients with up to 15 digits. The computation of the biggest system of study points S_c takes 4.5 minutes. On this example, study point boxes have to be refined up to a size of less than 2^{-255} to compute the topology. The following table gives the main characteristics of the study point systems :

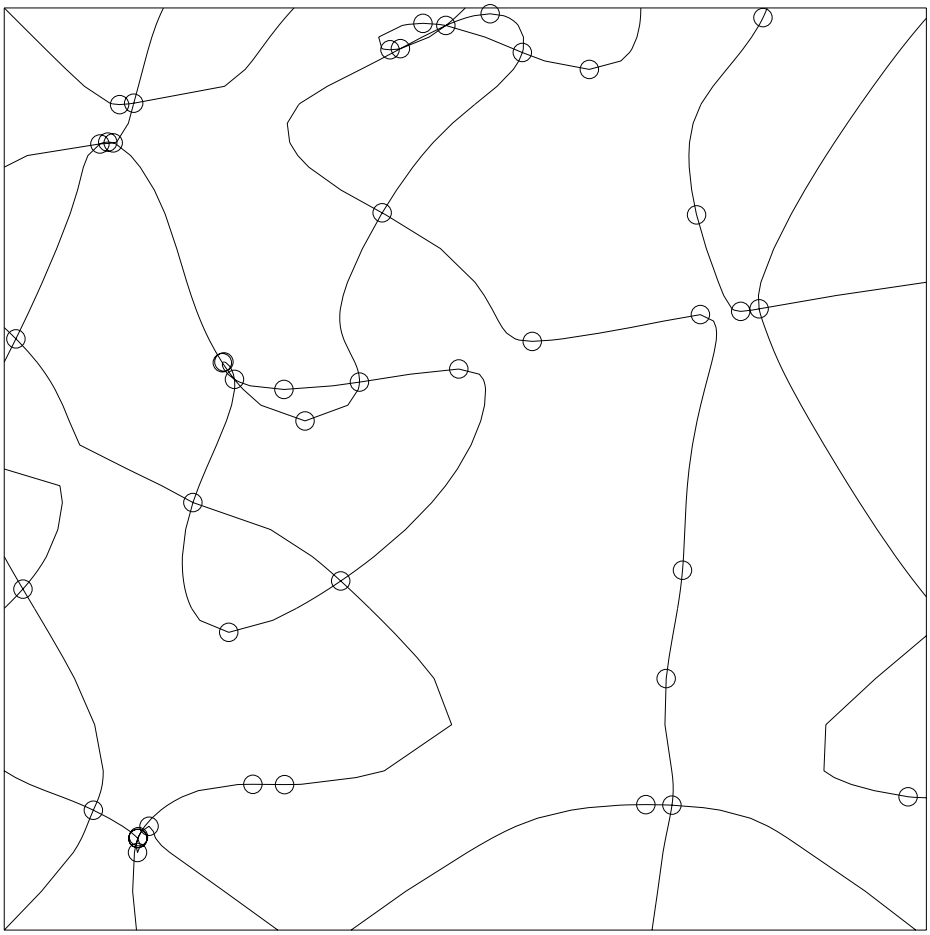

Fig. 4. Bi-quartic Bèzier example : isotopic approximation of the ridge curve with 3-ridge umbilics (green), 1-ridge umbilics (yellow), purple points (pink) and critical points (points with an horizontal tangent displayed in black).

System	# of roots $\in \mathbb{C}$	# of real roots $\in \mathcal{D}$
S_u	70	1
S_p	293	6
S_c	695	5

Figure 6 displays the topology of the ridges. In addition to study points, the regular points of all fibers are displayed as small black dots.

5 Conclusion

For parametric algebraic surfaces, we developed an algorithm to report a topologically certified approximation of the ridges. This algorithm is computationally demanding in

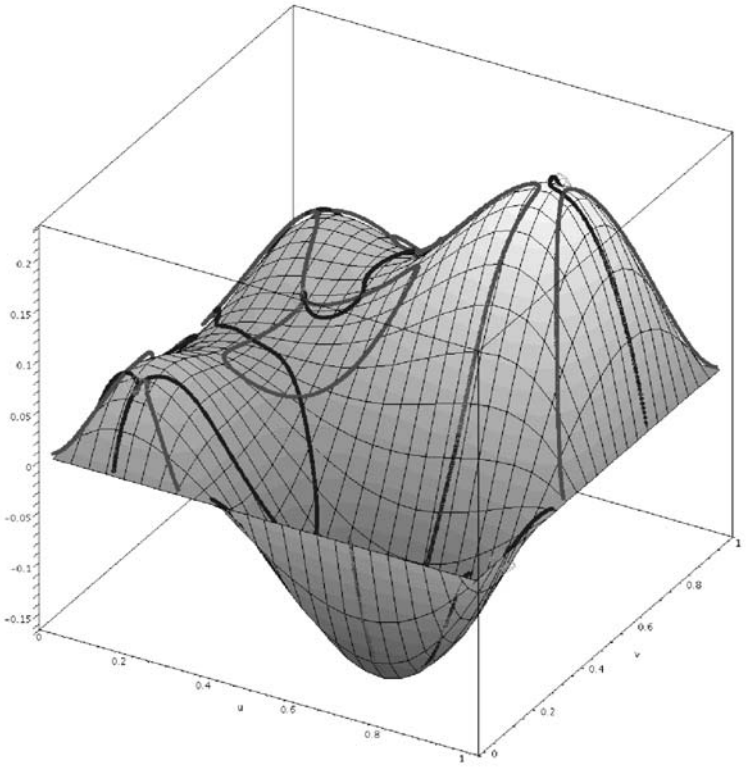

Fig. 5. Plot of the bi-quartic Bèzier surface with ridges and umbilics (boxed in green)

terms of algebra. It is in a sense complementary to the heuristic one developed in a companion paper [4], which is working directly on a triangulation of the surface, and provide a fast way to report non certified results.

The method developed for the computation of the topology of the ridges can be generalized for other algebraic curves. It gives an alternative to usual algorithms based on the CAD provided one knows the geometry of curve branches at singularities.

Acknowledgments

F. Cazals and M. Pouget acknowledge the support of the AIM@Shape and ACS European projects. Jean-Pierre Merlet is acknowledged for fruitful discussions.

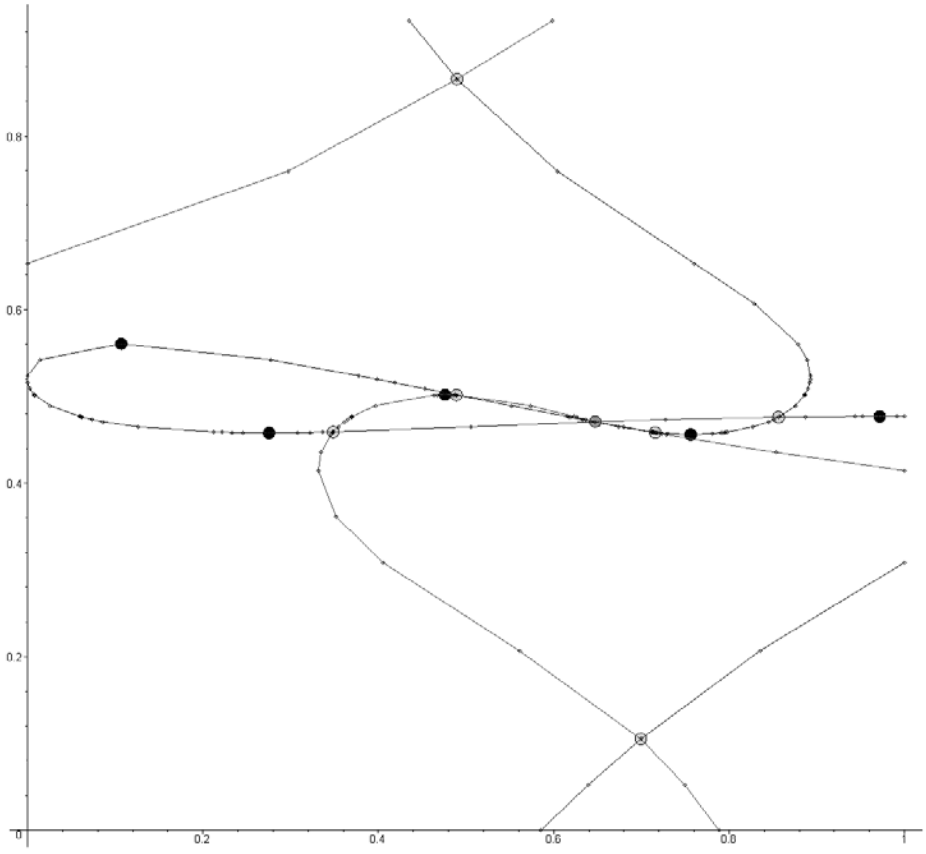

Fig. 6. Bi-quadratic Bèzier example : isotopic approximation of the ridge curve with the same color coding as in Fig. 4, in addition small black dots are regular points of all fibers.

References

1. D. Attali, J.-D. Boissonnat, and A. Lieutier. Complexity of the delaunay triangulation of points on surfaces the smooth case. In *ACM SoCG*, San Diego, 2003.
2. F. Cazals, J.-C. Faugère, M. Pouget, and F. Rouillier. Topologically certified approximation of umbilics and ridges on polynomial parametric surface. Technical Report 5674, INRIA, 2005.
3. F. Cazals, J.-C. Faugère, M. Pouget, and F. Rouillier. The implicit structure of ridges of a smooth parametric surface. *Computer Aided Geometrc Design*, 23(7):582–598, 2006.
4. F. Cazals and M. Pouget. Topology driven algorithms for ridge extraction on meshes. Technical Report RR-5526, INRIA, 2005.
5. J.-C. Faugère. A new efficient algorithm for computing gröbner bases (f_4). *Journal of Pure and Applied Algebra*, 139(1-3):61–88, June 1999.
6. J.-C. Faugère. A new efficient algorithm for computing gröbner bases without reduction to zero f_5. In *International Symposium on Symbolic and Algebraic Computation Symposium - ISSAC 2002, Villeneuve d'Ascq, France*, Jul 2002.

7. G. Gatellier, A. Labrouzy, B. Mourrain, and J.-P. Tècourt. Computing the topology of 3-dimensional algebraic curves. In *Computational Methods for Algebraic Spline Surfaces*, pages 27–44. Springer-Verlag, 2004.
8. J. Gravesen. Third order invariants of surfaces. In T. Dokken and B. Juttler, editors, *Computational methods for algebraic spline surfaces*. Springer, 2005.
9. L. Gonzalez-Vega and I. Necula. Efficient topology determination of implicitly defined algebraic plane curves. *Computer Aided Geometric Design*, 19(9), 2002.
10. D. Hilbert and S. Cohn-Vossen. *Geometry and the Imagination*. Chelsea, 1952.
11. P. W. Hallinan, G. Gordon, A.L. Yuille, P. Giblin, and D. Mumford. *Two-and Three-Dimensional Patterns of the Face*. A.K.Peters, 1999.
12. J.J. Koenderink. *Solid Shape*. MIT, 1990.
13. R. Morris. *Symmetry of Curves and the Geometry of Surfaces: two Explorations with the aid of Computer Graphics*. Phd Thesis, 1990.
14. R. Morris. The sub-parabolic lines of a surface. In Glen Mullineux, editor, *Mathematics of Surfaces VI, IMA new series 58*, pages 79–102. Clarendon Press, Oxford, 1996.
15. T. Maekawa, F. Wolter, and N. Patrikalakis. Umbilics and lines of curvature for shape interrogation. *Computer Aided Geometric Design*, 13:133–161, 1996.
16. X. Pennec, N. Ayache, and J.-P. Thirion. Landmark-based registration using features identified through differential geometry. In I. Bankman, editor, *Handbook of Medical Imaging*. Academic Press, 2000.
17. I. Porteous. The normal singularities of a submanifold. *J. Diff. Geom.*, 5, 1971.
18. I. Porteous. *Geometric Differentiation (2nd Edition)*. Cambridge University Press, 2001.
19. F. Rouillier. Solving zero-dimensional systems through the rational univariate representation. *Journal of Applicable Algebra in Engineering, Communication and Computing*, 9(5):433–461, 1999.
20. F. Rouillier and P. Zimmermann. Efficient isolation of polynomial real roots. *Journal of Computational and Applied Mathematics*, 162(1):33–50, 2003.
21. R. Seidel and N. Wolpert. On the exact computation of the topology of real algebraic curves. In *SCG '05: Proceedings of the twenty-first annual symposium on Computational geometry*, pages 107–115, New York, NY, USA, 2005. ACM Press.
22. J.-P. Thirion. The extremal mesh and the understanding of 3d surfaces. *International Journal of Computer Vision*, 19(2):115–128, August 1996.